Journal of Organometallic Chemistry 753 (2014) 72–80

Contents lists available at ScienceDirect

Journal of Organometallic Chemistry

journal homepage: www.elsevier.com/locate/jorganchem

Schiff base complexes of rare earth metal ions: Synthesis, characterization and catalytic activity for the oxidation of aniline and substituted anilines

L. Lekha [b], K. Kanmani Raja [c], G. Rajagopal [d], D. Easwaramoorthy [a,*]

[a] *Department of Chemistry, B.S. Abdur Rahman University, Vandalur, Chennai 600 048, Tamil Nadu, India*
[b] *Department of Chemistry, Saveetha School of Engineering, Thandalam, Chennai 602 105, Tamil Nadu, India*
[c] *Department of Chemistry, Government Arts College for Men (A), Nandanam, Chennai 600 035, Tamil Nadu, India*
[d] *Department of Chemistry, Madras Medical College, Chennai 600 003, Tamil Nadu, India*

ARTICLE INFO

Article history:
Received 5 November 2013
Received in revised form
29 November 2013
Accepted 5 December 2013

Keywords:
Schiff base
Amino acid
Lanthanide(III) Schiff base complexes
Fluorescence
Catalytic activity and oxidation of aniline

ABSTRACT

Several new lanthanide complexes of Pr(III), Sm(III), Gd(III), Tb(III), Er(III) and Yb(III) with the sodium salt of the Schiff base, 2-[(5-bromo-2-hydroxy-benzylidene)-amino]-5-methyl-pentanoic acid, derived from leucine and 5-bromosalicylaldehyde have been synthesized. These complexes having general formula $[Ln(HL)(NO_3)_2(H_2O)]\cdot NO_3$ were characterized by elemental analysis, UV–vis., FT-IR, EPR, Mass spectrometry and Thermal analysis. The FT-IR spectral data suggested that the ligand behaves as a tridentate ligand with one nitrogen and two oxygen donor atoms, sequence towards central metal ion. From the analytical data, the stoichiometry of the complexes was found to be 1:1 (metal:ligand). The physico-chemical data suggested eight coordination number for Ln(III) Schiff base complexes. Thermal behaviour (TGA/DTA) and fluorescence nature of the complexes were also studied. The Gd(III) Schiff base complex was found to be an efficient catalyst for the oxidation of aniline and substituted anilines under mild conditions.

1. Introduction

Schiff base ligands have gained paramount importance due to their versatility like straight forward synthesis, electron donor property and multidentate nature, which results in very high binding constants for d- and f-block metals [1,2]. The condensation between $-NH_2$ group of the amino acids and carbonyl group of the aldehydes or ketones needs a special condition due to Zwitter ionic effect of amino acids. It has been observed that pH plays a vital role in the process of condensation [3,4]. The trivalent lanthanide ion, complexes with strongly chelating species containing highly electronegative donor atoms, forms stable complexes [5]. Lanthanide and lanthanide complexes have attracted a great deal of interest in recent years because they have applications as antioxidants [6], in medicinal inorganic chemistry [7,8], catalysis [9], luminescence chemical probes and sensors [10] and pharmacological activities [11,12]. Further the lanthanide complexes were found to exhibit extremely sharp emission [13].

Catalytic oxidation has gained much interest among the academic and industrial chemists [14]. Especially, oxidation of organic substrates by inexpensive, readily abundant, terminal and environmental friendly oxidants like aqueous H_2O_2, molecular oxygen are very attractive from the view point of industrial technology and synthetic purposes [15]. Concerning the green oxidant, hydrogen peroxide is one of the most powerful candidates besides oxygen, because of its high atom efficiency, and water is expected as the only by-product to be generated from the reaction [16,17].

Catalytic oxidation of amines to their corresponding oxygen containing derivative has attracted much attention during the past few decades [18]. Only few examples have been reported [19,20], among which, it was found that transition-metal-catalyzed oxidative reaction of anilines to corresponding azobenzene is highly desirable under atmospheric conditions [21].

Anilines are most widespread and principal contaminants of industrial waste waters. These comprise an important class of environmental contaminants and they are the building blocks for many textile dyes, agrochemicals and other class of synthetic chemicals. The reaction pathways of aromatic amines in natural systems are dominated by redox reactions with soil and sediment

---

* Corresponding author. Tel.: +91 44 22751347x261, +91 9444075620 (mobile); fax: +91 4422750520.
E-mail addresses: easwaramoorthi@yahoo.com, easwar@bsauniv.ac.in (D. Easwaramoorthy).

0022-328X/$ – see front matter © 2013 Elsevier B.V. All rights reserved.
http://dx.doi.org/10.1016/j.jorganchem.2013.12.014

constituents. Oxidation of such compounds to harmless products is the important goal for basic research and industrial applications [22]. Oxidation of anilines leads to the formation of azobenzene [23], azoxybenzene [24,25], nitrobenzene [26] and nitrosobenzene [27] by organic [28] and inorganic oxidants [23]. The product composition in the oxygenation of amines depends on the oxidant, catalyst and reaction condition employed. The oxidation of aniline leading to the azo compound as a single product becomes a research interest for chemists.

As a result of the above facts, and in view of the diversified roles of lanthanide Schiff base metal complexes, in continuation of our work [29,30], we have synthesized and studied the physicochemical properties of lanthanide(III) complexes derived from Schiff base ligand with N, O donor atoms. The structures of the isolated complexes have been established using spectral techniques like UV–vis., FT-IR, ^{1}H NMR, Mass Spectrometry and EPR. The fluorescence study and investigation on the oxidation of aniline into their corresponding azobenzene in the presence of rare earth metal Schiff base complexes were made using H_2O_2 as an oxygen source.

2. Experimental

2.1. Materials

All the chemicals used were of analytical grade purchased from Aldrich chemical Company and were used without further purification.

2.2. Physical measurements

IR spectra (KBr pellets) were recorded in the region 4000–400 cm^{-1} on a FT-IR spectrum BX-II spectrophotometer. ^{1}H NMR spectrum was recorded with a model Bruker Advance DPZ-300 spectrometer operating at 300 MHz using DMSO-d_6 as a solvent and TMS as an internal standard. Electronic spectra were recorded on Perkin Elmer LS25 spectrophotometer using ethanol as a solvent. EPR spectra were recorded on an E4-EPR spectrometer. The measurements were taken in the X-band, on microcrystalline powder at liquid nitrogen temperature using DPPH as standard. The mass spectra were recorded on a GCMS-QP2010 Shimadzu mass spectrometer with DI (Direct Inlet) and CI (Chemical Ionization). Fluorescence spectra were measured in DMF using Perkin Elmer LS45 Fluorescence Spectrophotometer.

2.3. Synthesis of Schiff base ligand

The sodium salt of the Schiff base ligand was synthesized as per the following literature procedure [31]. To an aqueous solution of leucine (0.002 mol) in 10 mL water containing NaOH (0.002 mol), 5-bromosalicyaldehyde (0.002 mol) in 10 mL ethanol was added drop wise with constant stirring and heated under reflux for 3–5 h on a mantle at 50 °C. Then, the reaction mixture was cooled to room temperature. Fine shining yellow precipitate of the Schiff base ligand formed was filtered off, washed with ethanol–water mixture and stored in a vacuum desiccator over anhydrous calcium chloride.

2.4. Synthesis of $[Pr(HL)(NO_3)_2(H_2O)]\cdot NO_3$ complex

The rare earth Schiff base complex was synthesized as per the following general literature procedure [31]. A 0.002 mol of a Schiff base ligand was dissolved in 10 mL of ethanol. To this solution, a solution of 0.002 mol $Pr(NO_3)_3\cdot xH_2O$ in 10 mL water, was added drop wise with constant stirring and finally heated under reflux for 3–5 h on a hot plate at 50 °C. The reaction mixture was cooled to room temperature. A fine yellow precipitate of the solid complex formed was filtered off, washed with ethanol–water mixture and stored in a vacuum desiccator over anhydrous calcium chloride. All other Ln(III) complexes were prepared using the same procedure.

2.5. Procedure for oxidation of aniline

To a stirred solution of the catalyst (0.015 mmol) and 30% of H_2O_2 (10 mmol) in CH_2Cl_2 (7 mL), aniline (8 mmol) was added and the reaction mixture was stirred at room temperature for the required time. Progress of the reaction was monitored by TLC at regular intervals and continued for mentioned reaction time. After removal of the solvent, the residue was purified by Silica gel flash chromatography to afford azobenzene. All the azobenzene thus obtained were identified by comparing ^{1}H NMR data with values reported in the literature and those of the authentic samples. The desired 3,3′-azotoluene was obtained (yield: 66%), for which, ^{1}H NMR ($CDCl_3$, 200 MHz): δ (ppm) = 2.44 (s, 6H), 7.27–7.73 (m, 14H). ^{13}C NMR ($CDCl_3$, 100 MHz): δ (ppm) = 20.9, 119.7, 123.4, 128.7, 131.4, 138.0, 152.4.

3. Results and discussion

In the present investigation, the Schiff base ligand and its six new lanthanide metal complexes were synthesized and characterized by different analytical techniques. Scheme 1 summarizes the multi-step procedure leading to the target complexes. The ligand was synthesized by the one step condensation of leucine and 5-bromosalicyaldehyde and characterized by UV–vis., FT-IR, ^{1}H NMR, Mass and TG Analysis.

All the Ln(III) complexes were synthesized by the multi-step procedure in which $Ln(NO_3)_3\cdot xH_2O$ was used as the source of metal and they correspond to the formula $[Ln(HL)(NO_3)_2(H_2O)]\cdot NO_3$. All the complexes were stable in air and non-hygroscopic powders, soluble in DMSO, DCM and DMF, sparingly soluble in methanol, ethanol, acetonitrile and ethylacetate.

3.1. Elemental analysis

Table 1 shows the list of the elemental analysis of the Schiff base ligand and synthesized Ln(III) Schiff base complexes which are in good agreement with the calculated values.

A mass spectrum of the newly synthesized Schiff base ligand confirms the proposed formula by detecting the molecular fragments. Mass spectrometry chemical ionization of the ligand shows

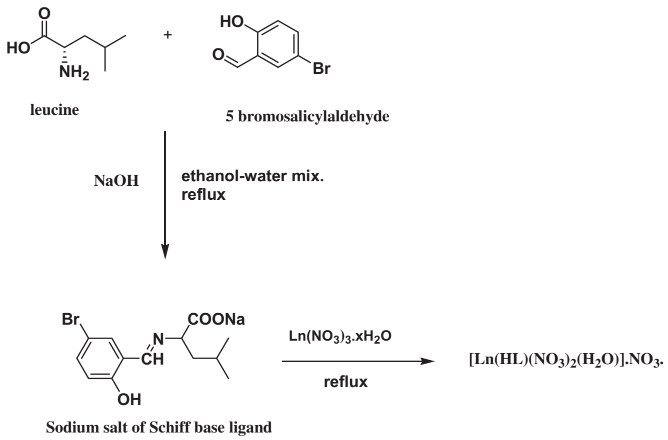

Scheme 1. Synthesis of Schiff base ligand and Ln(III) complexes.

Table 1
Elemental analysis of the ligand and Ln (III) Schiff base complexes.

Compound	*m*/*z*	Found (calc.)%			Colour	Yield (%)
		C	H	N		
Schiff base ligand	336	46.45(46.65)	4.50(4.49)	4.17(4.15)	Bright Yellow	86
$[Pr(HL)(NO_3)_2(H_2O)]NO_3$	596	26.16(26.18)	2.85(2.85)	7.03(7.04)	Yellow	96
$[Sm(HL)(NO_3)_2(H_2O)]NO_3$	605	25.75(25.76)	2.78(2.80)	6.93(6.93)	Yellow	94
$[Gd(HL)(NO_3)_2(H_2O)]NO_3$	612	25.48(25.47)	2.76(2.77)	6.84(6.85)	Yellow	96
$[Tb(HL)(NO_3)_2(H_2O)]NO_3$	613	25.40(25.40)	2.74(2.76)	6.85(6.84)	Yellow	95
$[Er(HL)(NO_3)_2(H_2O)]NO_3$	621	25.05(25.06)	2.74(2.73)	6.73(6.74)	Yellow	91
$[Yb(HL)(NO_3)_2(H_2O)]NO_3$	628	24.81(24.83)	2.69(2.70)	6.65(6.68)	Yellow	89

m/*z* at 336. The HRMS of the complexes show the molecular ions $[M]^{+\bullet}$ at various *m*/*z* values. Some isotopic peaks are also found around the fragment peaks [32].

3.2. Thermogravimetric analysis

The presence of water molecules and the thermal behaviour of the Schiff base ligand and the complexes were investigated by thermal analysis. Thermogravimetric curves, TGA and DTA for the ligand and $[Ln(HL)(NO_3)_2(H_2O)]\cdot NO_3$ complexes have been obtained in nitrogen atmosphere between 0 and 800 °C. Fig. 1 represents the TGA and DTA curves for Pr(III) Schiff base complex. The appearance of small endothermic peak on DTA curve around 100 °C corresponds to the loss of the water molecule [33]. The corresponding weight loss on TGA curve is 2.7% due to the release of water molecule. A further increase of temperature up to 200 °C, leads to the elimination of HNO_3 molecule, 28.31%. Further enhancement of temperature up to 400 °C leads to the decomposition of organic moiety with the weight loss of 40.23% [34]. The final residue of 28.76% corresponds to the Pr_2O_3 [35].

The thermal behaviour of the other lanthanide complexes is similar to $[Pr(HL)(NO_3)_2(H_2O)]\cdot NO_3$ which indicates that the complexes undergo two major steep degradation steps. In the first stage, the coordinated water molecules are eliminated followed by the elimination of nitric acid, the second stage decomposition corresponding to the elimination of the Schiff base ligand and beyond 640 °C the TGA curve show no change, possibly due to the complexes being decomposed to its corresponding Ln_2O_3 [35].

3.3. ^1H NMR spectra

The ^1H NMR Spectra of Schiff base ligand in DMSO-d_6 is shown in Fig. 2, which shows signal of multiplets at δ 0.84–0.88 ppm equivalent to the 6H of two methyl groups. Singlet at δ 1.69 ppm corresponds to the methine protons associated with two methyl groups. Multiplets at δ 2.43–2.56 ppm are due to α, β methylene hydrogen atom associated with an azomethine group [36]. The multiplets in δ 6.59–7.49 ppm region are assigned to the protons of the benzylidene ring groups [37]. The singlet at δ 3.32 ppm is due to the water impurity of the deuterated DMSO, and the strong singlet at δ 8.34 ppm is assigned to the azomethine proton [38]. This is in accordance with the IR data.

3.4. Spectroscopic characterization of the Schiff ligand and the Ln(III) complexes

The IR spectral data for the Schiff base ligand and Ln(III) complexes, are listed in Table 2 and representative spectrum of the complex is shown in Fig. 3. In order to study the binding mode of the Schiff base ligand to the metal ion in the complexes, the IR Spectrum of the free Schiff base ligand was compared with the spectra of the complexes. The change in profile of stretching frequencies in the complexes, while compared with those observed for the isolated ligand confirms the coordination of the ligand with the central metal ion. The IR spectral shifts of different complexes are similar, indicating similar structures of the Ln(III) complexes.

The IR spectrum of the ligand shows a strong absorption band around 1665 cm^{-1}, which may be attributed to the azomethine group and it was found that this absorption frequency shifted to 1640 cm^{-1} in the spectra of the complex indicates a stronger double bond character of the imine bond and a coordination of the azomethine nitrogen atom to the Ln(III) ion [39,40]. This coordination is further confirmed through the appearance of a medium intensity band around 420 cm^{-1} assigned to an Ln-N vibration. The IR spectrum of the free Schiff base ligand exhibits a broad band around 3400 cm^{-1}, which is attributed to the stretching frequency of the aromatic hydroxyl substituent group, perturbed by intramolecular hydrogen bonding [O–H⋯N] between phenolic hydrogen and

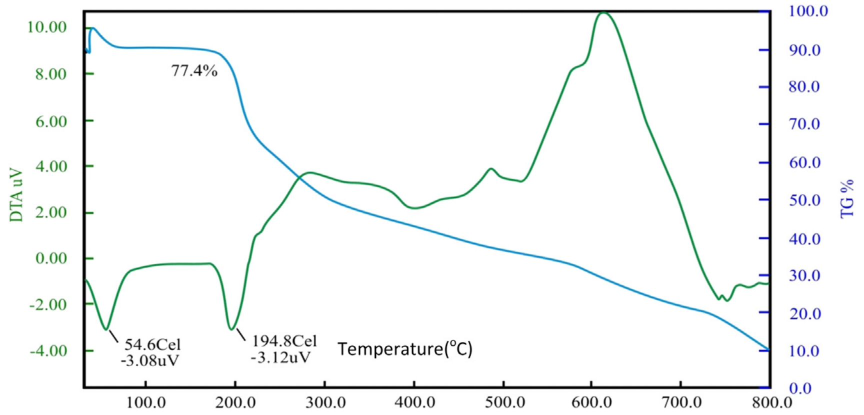

Fig. 1. Representative TG/DTA curves of the $[Pr(HL)(NO_3)_2H_2O]\cdot NO_3$ complex.

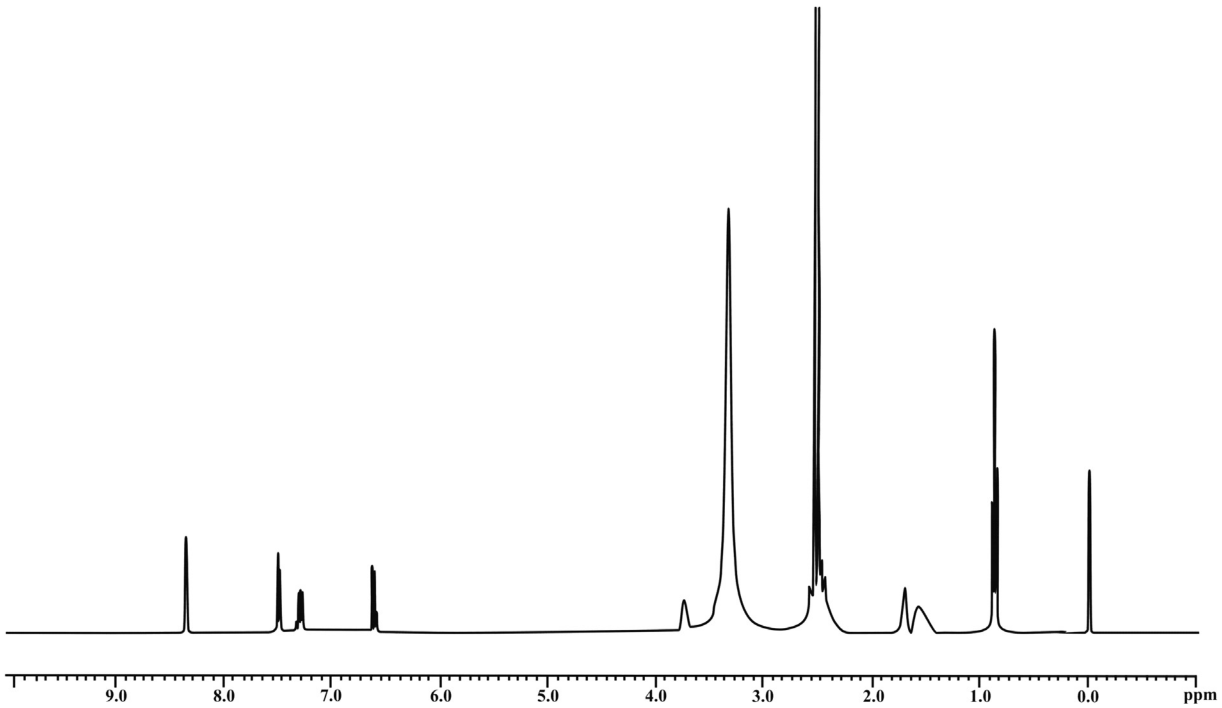

Fig. 2. ^{1}H NMR spectra of the Schiff base ligand.

Table 2
Significant infrared spectral data for the ligand and the Ln(III) complexes.

Compounds	ν_{OH}	$\nu_{C=N}$	ν_{Ar-O}	$\nu_{NO_3^-}$					$\nu_{asym\ (COO^-)}$	$\nu_{sym\ (COO^-)}$	ν_{Ln-O}	ν_{Ln-N}
				ν_1	ν_2	ν_3	ν_4	ν_0				
Schiff base ligand	3400	1665	1260	–	–	–	–	–	–	–	–	–
$[Pr(HL)(NO_3)_2(H_2O)]NO_3$	3490	1640	1268	1470	1028	825	1290	1383	1505	1380	540	420
$[Sm(HL)(NO_3)_2(H_2O)]NO_3$	3485	1642	1270	1471	1029	827	1292	1383	1515	1390	548	421
$[Gd(HL)(NO_3)_2(H_2O)]NO_3$	3495	1640	1270	1470	1029	825	1290	1383	1505	1380	545	420
$[Er(HL)(NO_3)_2(H_2O)]NO_3$	3492	1638	1268	1471	1028	826	1292	1383	1500	1380	540	422
$[Tb(HL)(NO_3)_2(H_2O)]NO_3$	3480	1641	1270	1470	1028	825	1292	1383	1510	1390	546	420
$[Yb(HL)(NO_3)_2(H_2O)]NO_3$	3498	1640	1270	1470	1029	826	1292	1383	1525	1400	545	418

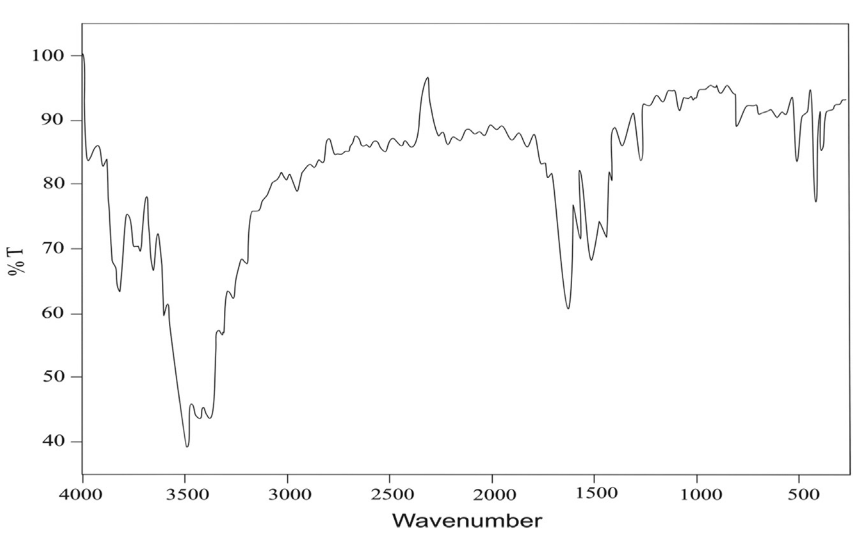

Fig. 3. IR Representative spectrum of $[Yb(HL)(NO_3)_2H_2O]\cdot NO_3$complex.

azomethine nitrogen atoms [41,42]. Further, the appearance of the –OH band around 3490 cm^{-1} in the spectra of the complexes with an increase in intensity indicates that the hydroxyl oxygen is coordinated to the Ln(III) ion without proton displacement [43]. The appearance of band near 1260 cm^{-1} in the free Schiff base ligand is associated with the Ar–O band of the phenolic hydroxyl substituent [44]. The shift in the stretching frequency of Ar–O band around 1270 cm^{-1} in the spectra of the Ln(III) complexes suggest the coordination of Ln(III) ion occurs through the oxygen atom of the hydroxyl benzene of the Schiff base ligand [45]. The complexes show a strong band in the region 1500–1525 cm^{-1} and a weaker band in the region 1380–1400 cm^{-1} assigned to asymmetric and symmetric stretching frequencies of COO$^-$ group respectively. The frequency difference between the asymmetric and symmetric stretching frequencies comes around 215 cm^{-1}, which suggests the monodentate coordination of the carboxyl group of amino acid with the Ln(III) ion [46]. This is further confirmed through the appearance of a medium intensity band around 540 cm^{-1}, which may be assigned to Ln–O vibration [47]. The infrared spectra of the Ln(III) complexes displays several intense band at 1470 cm^{-1} (ν_1), 1028 cm^{-1} (ν_2), 825 cm^{-1} (ν_3) and 1290 cm^{-1} (ν_4), which represents the coordinated nitrate ions with the central metal ion. The difference in frequency separation is approximately 180 cm^{-1}, which suggests that the mode of coordination of NO_3^- ion with the central metal ion is bidentate in nature [48,49]. The IR band at 1383 cm^{-1} in the spectrum of the complex indicates the existence of the free nitrate group in the coordination sphere. The existence of medium intensity band around 1615 cm^{-1} is due to the symmetric and the asymmetric O–H stretching vibrations of inner-sphere water molecule [50]. The presence of coordinated water is also established and supported by TG/DTA analysis of these complexes.

Electron Paramagnetic Resonance is being a very powerful method of studying the magnetic properties and crystal field symmetry of the lanthanide(III) complexes. Since, spin-lattice relaxation times are shortened due to the very strong spin–orbit coupling in Ln(III) ion, the EPR spectra can be observed at very low temperature. The X-band EPR spectrum of the $[Gd(HL)(NO_3)_2(H_2O)]\cdot NO_3$ complex exhibits the following lines with effective g values of 4.55, 2.12 and 1.64, which represents $g_x \neq g_y \neq g_z$; shows the rhombic spectral nature of $[Gd(HL)(NO_3)_2(H_2O)]\cdot NO_3$ complex [51]. As a result, the transition of unpaired electron between these split levels with $g \geq 2$ and $g < 2$ are observed. The presence of these lines indicates the case of the existence of a strong crystal field.

Table 3
UV–vis. spectral data λ_{max} (nm) for the ligand and the complexes.

Compound	λ_{max} (nm)	$\varepsilon \times 10^4$(cm^2 mol^{-1})	Band assignment
Schiff base ligand	203,241,334	5.05,4.52,3.28	$\pi \rightarrow \pi^*$
	424	1.61	$n \rightarrow \pi^*$
$[Pr(HL)(NO_3)_2(H_2O)]NO_3$	200,229,364	3.58,2.41,0.31	$\pi \rightarrow \pi^*$
	273	0.47	LMCT
	429	0.05	$n \rightarrow \pi^*$
$[Sm(HL)(NO_3)_2(H_2O)]NO_3$	202,242,359	3.17,0.79,0.15	$\pi \rightarrow \pi^*$
	280	0.20	LMCT
	442	0.07	$n \rightarrow \pi^*$
$[Gd(HL)(NO_3)_2(H_2O)]NO_3$	200,230,369	3.40,1.36,0.0	$\pi \rightarrow \pi^*$
	276	0.34	LMCT
	428	0.094	$n \rightarrow \pi^*$
$[Tb(HL)(NO_3)_2(H_2O)]NO_3$	201,229,361	4.09,3.30,0.52	$\pi \rightarrow \pi^*$
	273	0.7	LMCT
	433	0.085	$n \rightarrow \pi^*$
$[Er(HL)(NO_3)_2(H_2O)]NO_3$	203,229,364	3.58,1.59,0.21	$\pi \rightarrow \pi^*$
	273	0.34	LMCT
	429	0.05	$n \rightarrow \pi^*$
$[Yb(HL)(NO_3)_2(H_2O)]NO_3$	200,222,339	3.49,1.77,0.21	$\pi \rightarrow \pi^*$
	252	0.83	LMCT
	407	0.071	$n \rightarrow \pi^*$

The UV–vis. absorption spectra for the Schiff base ligand and the Ln(III) complexes were carried out in DMF at room temperature. The numerical values of the maximum absorption wavelength (λ_{max}) are listed in Table 3 and shown in Fig. 4. The absorption of the ligand is characterized by four main absorption bands in the regions 200–500 nm. The band at the $\lambda_{max} = 203$ nm and at 241 nm is attributed to $\pi \rightarrow \pi^*$ transition state [52,53]. The band at the $\lambda_{max} = 334$ nm corresponds to the $\pi \rightarrow \pi^*$ transition state of the azomethine group and the $\lambda_{max} = 424$ nm is attributed to the $n \rightarrow \pi^*$ transition state associated with the azomethine group with an intra-molecular charge transfer [44].

The UV spectra of the complexes generally show the characteristic bands of the free ligands with some changes both in

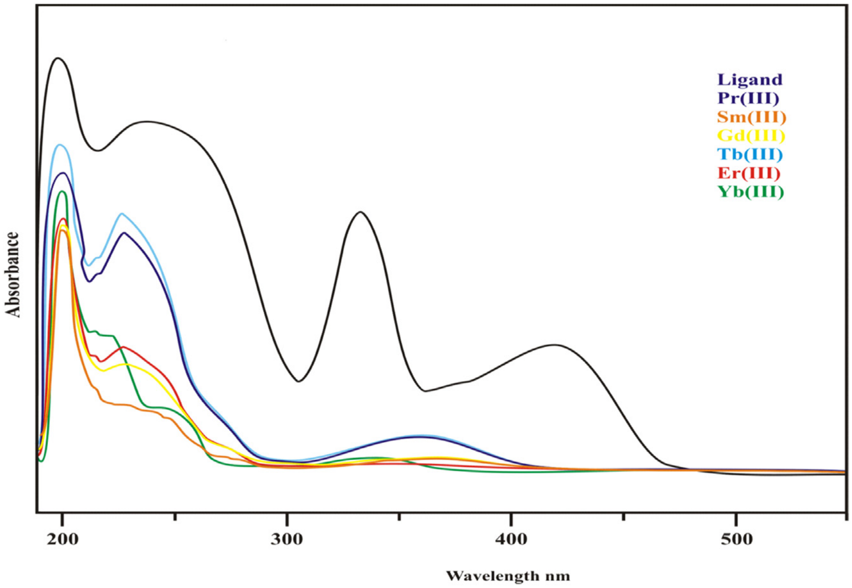

Fig. 4. UV spectra of the Schiff base ligand and Ln(III) Schiff base complexes in DMF solution (1.0×10^{-6} M) at room temperature.

frequencies and intensities. These modifications of the shifts and the intensity of the absorption bands confirmed the coordination of the ligand to the metal ion. The UV–vis. absorption spectra of all the Ln(III) Schiff base complexes show similarities, which indicates similarity in their structures. In general, the lanthanide ions do not appreciably contribute to the spectra of their complexes, since f–f transitions are Laporte-forbidden and very weak in nature [54]. The absorption bands around 200, 330, 420 nm are slightly shifted to lower frequencies upon complexation. The appearance of a new band around 270 nm, being absent in the ligand gives further evidence for the complexation. The band at 273 nm is attributed to the ligand metal charge transfer [55] and the one around 360 nm may assigned to the $\pi \rightarrow \pi^*$ transition state of the azomethine group coupled with charge transfer from ligand to central metal ion [56].

Photophysical studies of the ligand and its rare earth metal complexes have been explored in this article. Fig. 5 gives the emission spectrum of the Samarium and Terbium Schiff base complexes in DMF solution at room temperature. Fluorescence properties refer to any process, which increases, decreases the fluorescence intensity or a shift of the maximum absorption of a sample. These include excited state reaction, molecular rearrangement, energy transfer, ground state complex formation and quenching due to collision [34].

The emission spectra of the complexes were recorded upon the excitation at 395 nm. The ligand present fluorescence band at 485 nm. The fluorescence spectra of the complexes present bands that indicate the formation of complexes and fluorescence property of the metallic ions. The strongest emission was located around 485 nm for the free ligand, may be attributed to $\pi \rightarrow \pi^*$ transition state, which shifts upon the complexation. Due to the shielding of 4f orbitals from the environment by an outer shell of 5s and 5p orbitals, the f–f absorption bands are very narrow, which causes the minimally perturbed spectral properties of the lanthanide ions by the external field generated by the ligands [57]. An organic ligand is necessary to improve the quantum yield of luminescent emission for the lanthanide ions, since the absorption coefficients of the ligand are many orders of magnitude larger than the intrinsically low molar absorption coefficients of the trivalent lanthanide ions [58]. Besides, the direct coordination of an organic ligand to a lanthanide ion can further improve the energy-transfer rates by reducing the distance between the ligand and the lanthanide ion [59,60]. This energy excites the ligand to the excited singlet (S^1) state, followed by an energy migration via intersystem crossing from the S^1 state to a ligand triplet (T) state. The energy is then transferred from the triplet state of the ligand to a resonance state of the coordinated lanthanide ion without radiation, which in turn undergoes subsequent emission in the visible region [61–64].

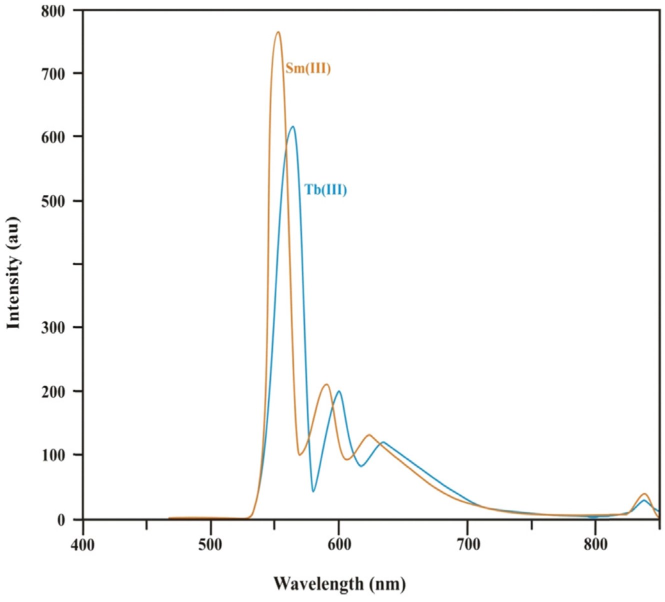

Fig. 5. Emission spectra of Sm(III) and Tb(III) Schiff base complexes in DMF solution (1.0×10^{-6} M) at room temperature. Emission spectrum is obtained with $\lambda_{exc.} = 395$ nm.

Inspection of emission spectra at $\lambda_{exc.}$ 395 nm exhibits the characteristic emission spectra of Sm(III) and Tb(III) complexes. This indicates the coordination nature of the ligand with rare earth metal (III) ions for absorption and transfer of energy. The sensitized emission spectra of Sm(III) Schiff base complexes display two luminescence bands at 565 nm and 600 nm corresponding to the ${}^4G_{5/2} \rightarrow {}^6H_{5/2}$ and ${}^4G_{5/2} \rightarrow {}^6H_{7/2}$ respectively and a shoulder at 642 nm is due to ${}^4G_{5/2} \rightarrow {}^6H_{9/2}$. Similarly, the Tb(III) Schiff base complexes also display two fluorescence bands around 556 nm and 590 nm, this may attributed to ${}^5D_4 \rightarrow {}^7F_5$ and ${}^5D_4 \rightarrow {}^7F_4$ respectively and a shoulder at 624 nm due to ${}^5D_4 \rightarrow {}^7F_3$. This indicates that the energy-transfer chain is successfully completed from the excitation of the ligand to the emission of the coordinated Sm(III) and Tb(III) central metal ions [52]. The appearance of small band at 840 nm denotes the secondary derivatives of the rare earth Schiff base complexes.

3.5. Catalytic oxidation of aniline

The oxidation of aniline and its derivatives to the corresponding azo compound have been carried out smoothly in an almost quantitative yield using H_2O_2 as an oxidant and rare earth metal Schiff base complexes as catalyst.

Table 4 gives the results of aniline oxidation into their corresponding azobenzene as the product. All the reactions were carried out at room temperature, by using 30% H_2O_2 as an oxidant combined with the catalytic amount of rare earth metal Schiff base complexes. The azobenzene was produced in good yield at room temperature in CH_2Cl_2 with the reaction time less than an hour.

Initially, the reaction was carried out without catalyst (Table 4, entry 1) and enhanced amount of oxidant, it proceeds with the formation of product with poor yield and greater reaction time. Then six types of catalyst were tested (Table 4, entries 2–7), 70–90% yields of azobenzene with excellent conversions were obtained. To our surprise, among the various catalyst used, the conversion of aniline to corresponding azobenzene in the presence of $[Gd(HL)(NO_3)_2(H_2O)]NO_3$ with 10 mmol of H_2O_2, results 85% of yield within 15 min of reaction time at reflux (Table 4, entry 3). Elevation of reaction temperature has no effect on the aniline oxidation with the above Gd(III) Schiff base complex as a catalyst. The other tested catalyst also gave moderate to good yield of oxidation product (Table 4, entries 4–6). Although, the $[Sm(HL)(NO_3)_2(H_2O)]NO_3$ and

Table 4
Oxidation of aniline catalyzed by various Ln(III) complexes in CH_2Cl_2 at RT.

Entry	Catalyst	Oxidant	Yield (%)	Reaction time (min)
1	–	Enhanced conc. H_2O_2	30	180
2	$[Sm\,(HL)\,(NO_3)_2(H_2O)]NO_3$	H_2O_2	90	30
3	$[Gd\,(HL)\,(NO_3)_2(H_2O)]NO_3$	H_2O_2	85	15
4	$[Pr\,(HL)\,(NO_3)_2(H_2O)]NO_3$	H_2O_2	70	25
5	$[Eu\,(HL)\,(NO_3)_2(H_2O)]NO_3$	H_2O_2	80	30
6	$[Tb\,(HL)\,(NO_3)_2(H_2O)]NO_3$	H_2O_2	75	25
7	$[Yb\,(HL)\,(NO_3)_2(H_2O)]NO_3$	H_2O_2	90	60
8	$[Gd\,(HL)\,(NO_3)_2(H_2O)]NO_3$	–	–	240

Table 5
Oxidation of aniline and substituted anilines catalyzed by Gd(III) complex in CH_2Cl_2 at RT.

Entry	Anilines	Product	Yield (%)
1	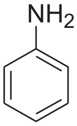 Phenylamine	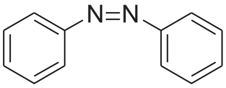 Diphenyl-diazene	85
2	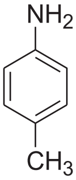 *p*-Tolylamine	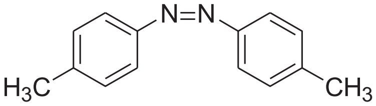 Di-*p*-tolyl-diazene	88
3	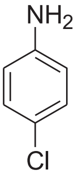 4-Chloro-phenylamine	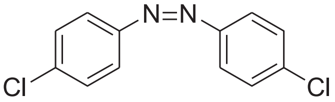 Bis-(4-chloro-phenyl)-diazene	30
4	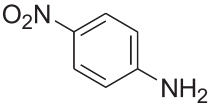 4-Nitro-phenylamine	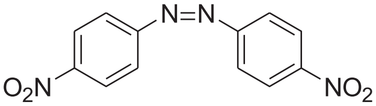 Bis-(4-nitro-phenyl)-diazene	12
5	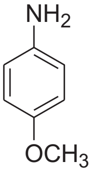 4-Methoxy-phenylamine	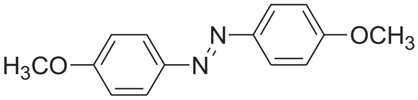 Bis-(4-methoxy-phenyl)-diazene	88
6	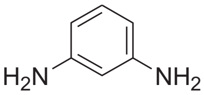 m-phenylenediamine	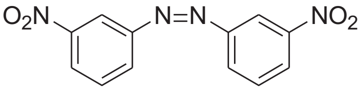 Bis-(3-nitro-phenyl)-diazene	60
7	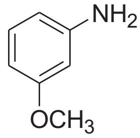 3-Methoxy-phenylamine	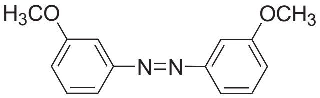 Bis-(3-methoxy-phenyl)-diazene	62
8	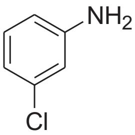 3-Chloro-phenylamine	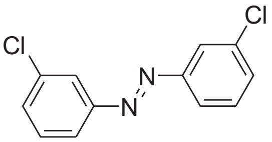 Bis-(3-chloro-phenyl)-diazene	20

Table 5 (*continued*)

Entry	Anilines	Product	Yield (%)
9	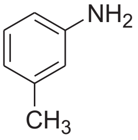 *m*-Tolylamine	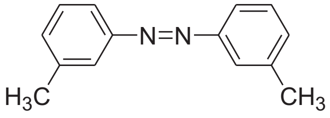 Di-*m*-tolyl-diazene	66
10	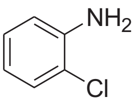 2-Chloro-phenylamine	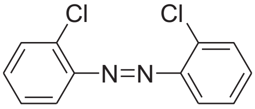 Bis-(2-chloro-phenyl)-diazene	12
11	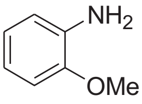 2-Methoxy-phenylamine	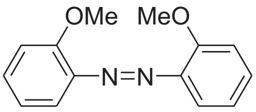 Bis-(2-methoxy-phenyl)-diazene	25
12	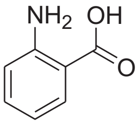 Amino-benzoic acid	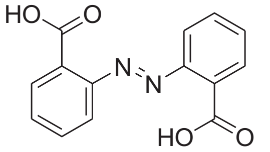 azodibenzoicacid	12

$[Yb(HL)(NO_3)_2(H_2O)]NO_3$ complexes gave the good yield of the product (90%), the reaction time (30 min and 60 min respectively) was the fact that carries less importance in the purview of industrial and academics. The effect of catalyst without oxidant (Table 4, entry 8) was also tested. No starting material was converted into the product in the absence of H_2O_2. After these testing, $[Gd(HL)(NO_3)_2(H_2O)]NO_3$ was chosen as the catalyst and 10 mL of H_2O_2 as an oxidant as the best reaction conditions.

To our delight 85% of azobenzene was produced in CH_2Cl_2 with total conversion of staring material and only 2 mol % of catalyst were utilized for the oxidation purpose. With the best reaction condition (Table 4, entry 3) the experiment was carried out to check the generality and efficiency of this methodology with the various kinds of substituted anilines are shown in Table 5. Under the optimized conditions, aniline (entry 1) and various substituted anilines were oxidized to its corresponding products in good to excellent yields. The oxidative reaction of aromatic aniline with an electron withdrawing substituted group such as nitro, acid and chloro group on the phenyl ring proceeds with the yield of trace amount (entries 3, 4, 8, 10 and 12) under the reaction conditions. This was suspected due to the low electron density of phenyl ring. Further, among the various ortho, meta and para substituted anilines, para substituted anilines results excellent yield of the oxidative products (entries 2 and 5) while compared with meta substituted aniline, which results good yield of the desired product (entries 6, 7 and 9) and ortho substituted aniline, which results a moderate yield of the desired product (entry 11). The desired products were characterized by ^1H NMR.

In summary, a general rare earth metal Schiff base catalyzed oxidation of aniline and substituted aniline to the corresponding azo compounds have been developed. The reaction proceeds at room temperature and use H_2O_2 as the green oxidant, provides a simple and general procedure for the preparation of azo derivatives that is difficult to prepare by conventional methods. The result clearly demonstrates that this oxidation system is more efficient in the oxidation of aniline to azobenzene with H_2O_2 as an oxidant and $[Gd(HL)(NO_3)_2(H_2O)]\cdot NO_3$ complex as a catalyst.

4. Conclusion

In this work the tridentate Schiff base ligand and its Ln(III) complexes of the type $[Ln(HL)(NO_3)_2(H_2O)]\cdot NO_3$ were synthesized and characterized by elemental analysis, TGA/DTA, spectral analysis like ^1H NMR, UV, FT-IR, EPR and Mass Spectrometry. These analytical and spectral data reveal that the ligand coordinate to the central Ln(III) ion by its phenolic oxygen, azomethine nitrogen and the carboxylic oxygen with 1:1 stoichiometry and their coordination number is eight. The samarium and terbium complexes present interesting fluorescence properties. The newly prepared Ln(III) complexes possesses good catalytic ability for oxidation of aniline under mild conditions and $[Gd(HL)(NO_3)_2(H_2O)]\cdot NO_3$ complex was utilized to check the generality and efficiency of oxidation of various substituted anilines.

Acknowledgements

The authors thank the authorities of B.S. Abdur Rahman University, Chennai 600048, The Dean, Madras Medical College, Government Rajivgandhi General Hospital, Chennai 600003, Saveetha School of Engineering, Chennai and Department of Chemistry, Government Arts College for Men (A), Nandanam, Chennai 600 035, for providing research facilities and moral support.

References

[1] S. Salehzadeh, S.M. Nouri, H. Keypour, M. Bagherzadeh, Polyhedron 24 (2005) 1478.
[2] M. Andruh, F. Tuna, in: M.A. Cato (Ed.), Focus on Organometallic Chemistry Research, Nova Publishers, Hauppauge, 2005.
[3] N.A. Nawar, A.M. Shallaby, N.M. Hosny, M. Mostafa, Trans. Met. Chem. 26 (2001) 180.
[4] N.M. Hosny, Trans. Met. Chem. 32 (2007) 117.
[5] F.B. Tamboura, P.M. Haba, M. Gaye, A.S. Sall, A.H. Barry, T. Jouini, Polyhedron 23 (2004) 1191.
[6] M.-F. Wang, Z.-Y. Yang, Z.-C. Liu, Y. LI, T.-R. Li, M.-H. Yan, X.-Y. Cheng, J. Coord. Chem. 65 (2012) 3805.
[7] L. Thunus, R. Lejeune, Coord. Chem. Rev. 184 (1999) 125.
[8] C.S. Cutler, C.J. Smith, G.J. Ehrhardt, T.T. Tyler, S.S. Jurisson, E. Deutsch, Cancer Biother. Radiopharm. 15 (2000) 531.
[9] Z. Li, M. Xue, H. Yao, H. Sun, Y. Zhang, Q. Shen, J. Organomet. Chem. 713 (2012) 27.
[10] T.-L. Yang, W.-W. Qin, Spectrochim. Acta Part A 67 (2007) 568.
[11] M. Wang, Z. Yang, Y. Li, H. Li, J. Coord. Chem. 64 (2011) 2974.
[12] P.R. Reddy, A. Shilpa, N. Raju, P. Raghavaiah, J. Inorg. Biochem. 15 (2011) 1603.
[13] M.R. Robinson, M.B. O'Regan, Bazan, Chem. Commun. (2000) 1645.
[14] A.E. Shilov, G.B. Shul'pin, Chem. Rev. 97 (1997) 2879.
[15] A.H. Hains, Methods for the Oxidation of Organic Compounds, Academic, London, 1985.
[16] N. Mizuno, K. Yamaguchi, K. Kamata, Coord. Chem. Rev. 249 (2005) 1944.
[17] R. Ramnauth, S. Al-Juaid, B.C. Parkin, A.C. Sullivan, Inorg. Chem. 43 (2004) 4072.
[18] V.K. Ahluwalia, Organic Reaction Mechanisms, Parashar Publisher CRC Press, New Delhi, 2002.
[19] J.S.M. Samec, A.H. Ell, J.-E. Bäckvall, Chem. Eur. J. 11 (2005) 2327.
[20] S. Satoru, M. Miura, M. Nomura, J. Org. Chem. 54 (1989) 4700.
[21] W. Lu, C. Xi, Tetrahedron Lett. 49 (2008) 4011.
[22] S.S. Mansoor, S.S. Shafi, S.J. Ahmed, Arabian J. Chem. (2010) in press, http://dx.doi.org/10.1016/j.arabjc.2013.02.005.
[23] O.D. Wheeler, D. Gonzales, Tetrahedron 20 (1964) 189.
[24] A. Nezhadali, M. Akbarpour, Chin. Chem. Lett. 21 (2010) 43.
[25] R. Zhao, C. Tan, Y. Xie, C. Gao, H. Liu, Y. Jiang, Tetrahedron Lett. 52 (2011) 3805.
[26] R.W. White, W.D. Emmons, Tetrahedron 17 (1962) 31.
[27] H.E. Baumgarten, A. Staklis, E.M. Miller, J. Org. Chem. 30 (1965) 1203.
[28] W.D. Emmons, J. Am. Chem. Soc. 79 (1957) 5528.
[29] L. Lekha, K. Kanmani Raja, G. Rajagopal, D. Easwaramoorthy, J. Mol. Struct. 1056–1057 (2014) 307.
[30] K.K. Raja, D. Easwaramoorthy, S.K. Rani, J. Rajesh, Y. Jorapur, S. Thambidurai, P.R. Athappan, G. Rajagopal, J. Mol. Catal. A Chem. 303 (2009) 52.
[31] P. Gawryszewska, J. Lisowski, Inorg. Chim. Acta 383 (2012) 220.
[32] S.M. Schildcrout, S. SriHari, J. Masnovi, Inorg. Chem. 64 (1995) 4117.
[33] L. Guo, B. Yan, J. Photochem. Photobiol. A Chem. 224 (2011) 141.
[34] A. Pui, T. Malutan, L. Tataru, C. Mualtuan, D. Humelnicu, G. Carja, Polyhedron 30 (2011) 2127.
[35] X. Li, C.Y. Wang, H.-M. Hu, Inorg. Chem. Commun. 11 (2008) 345.
[36] N. Raman, K. Pothiraj, T. Baskaran, J. Mol. Struct. 1000 (2011) 135.
[37] C.R. Bhattacharieea, P. Goswami, H.A.R. Pramanika, P.C. Paula, P. Mondal, Spectrochim. Acta Part A 78 (2011) 1408.
[38] P.R. Shakya, A.K. Singh, T.R. Rao, Spectrochim. Acta Part A 79 (2011) 1654.
[39] G. Leniec, S.M. Kaczmarek, J. Typek, B. Kołodziej, E. Grech, W. Schilf, J. Phys. Condens. Matter 18 (2006) 9871.
[40] S.M. Kaczmarek, G. Leniec, J. Non-Cryst. Solids 355 (2009) 1325.
[41] M. Salavati-Niasari, Z. Salimi, M. Bazarganipour, F. Davar, Inorg. Chim. Acta 362 (2009) 3715.
[42] D.N. Kumar, B.S. Garg, Spectrochim. Acta Part A 64 (2006) 141.
[43] A.M. Ajlouni, Z.A. Taha, W.A. Momani, A.K. Hijazi, M. Ebqa'ai, Inorg. Chim. Acta. 388 (2012) 120.
[44] T.A. Youssef, J. Coord. Chem. 61 (2008) 816.
[45] W.B. Sun, P.F. Yan, G.M. Li, H. Xu, J.W. Zhang, J. Solid State Chem. 182 (2009) 381.
[46] G.B. Deacon, R.J. Phillips, Coord. Chem. Rev. 33 (1980) 227.
[47] L.J. Bellamy, The Infrared Spectra of Complex Molecules, J. Wiley, New York, 1971.
[48] P. Yan, W. Sun, Z. Li, C. Net, T. Gao, Z. Yue, J. Coord. Chem. 60 (2007) 1973.
[49] W. Wang, Y. Huang, N. Tang, Spectrochim. Acta 66 (2007) 1058.
[50] J.P. Costes, J. Laussac, F. Nicodeme, J. Chem. Soc., Dalton Trans. 2731 (2002).
[51] A. Szyczewki, S. Lis, J. Krzystek, K. Staninski, A. Klomlowski, Z. Kruczynski, M. Pietraszkiewick, J. Alloys Compd. 451 (2008) 182.
[52] L. Guo, S. Wu, F. Zeng, J. Zhao, Eur. Polym. J. 42 (2006) 1670.
[53] R.C. Felico, E.T.G. Canalheiro, E.R. Dockal, Polyhedron 20 (2001) 261.
[54] C.G. Walrand, K. Binnemans, Handbook on the Physics Chemistry of Rare Earths, vol. 25, North-Holland Publishers, Amsterdam, 1998, p. 101.
[55] W. Xie, M.J. Heeg, P.G. Wang, Inorg. Chem. 38 (1999) 2541.
[56] M.M. Moawad, W.G. Hanna, J. Coord. Chem. 55 (2002) 439.
[57] N. Sabbatini, M. Guardigli, J.M. Lehn, Coord. Chem. Rev. 123 (1993) 201.
[58] S. Wu, F. Zeng, S. Wu, S. Yao, W. She, D. Luo, J. Mater. Sci. 38 (2003) 401.
[59] D.L. Dexter, J. Chem. Phys. 21 (1953) 836.
[60] A.G. Kolchinski, Coord. Chem. Rev. 174 (1998) 207.
[61] A.V. Haynes, H.G. Drickamer, J. Chem. Phys. 76 (1982) 114.
[62] K. Inoue, Y. Sasaki, T. Itaya, Eur. Polym. J. 33 (1997) 841.
[63] C.X. Du, L. Ma, Y. Xu, Eur. Polym. J. 34 (1998) 23.
[64] D.H. Kim, H.I. Cho, T. Zyung, Eur. Polym. J. 38 (2002) 133.